



City Research Online

City, University of London Institutional Repository

Citation: Thomaidis, I. M., Camara, A. and Kappos, A. J. (2017). Simulating the Response of Free-Standing Rocking Rigid Blocks using Abaqus/Standard. Paper presented at the 2017 SIMULIA UK Regional User Meeting, October 18 - 19, 2017, Cheshire, UK.

This is the accepted version of the paper.

This version of the publication may differ from the final published version.

Permanent repository link: <https://openaccess.city.ac.uk/id/eprint/18697/>

Link to published version:

Copyright: City Research Online aims to make research outputs of City, University of London available to a wider audience. Copyright and Moral Rights remain with the author(s) and/or copyright holders. URLs from City Research Online may be freely distributed and linked to.

Reuse: Copies of full items can be used for personal research or study, educational, or not-for-profit purposes without prior permission or charge. Provided that the authors, title and full bibliographic details are credited, a hyperlink and/or URL is given for the original metadata page and the content is not changed in any way.

Simulating the Response of Free-Standing Rocking Rigid Blocks using Abaqus/Standard

Ioannis M. Thomaidis^a, Alfredo Camara^a, Andreas J. Kappos^{a,b}

^a *Research Centre for Civil Engineering Structures, Civil Engineering Department, City, University of London, London, EC1V 0HB, United Kingdom*

^b *Civil Engineering Department, Aristotle University of Thessaloniki, Thessaloniki, GR 54124*

Abstract: This work presents detailed finite element models developed in Abaqus/Standard to study the rocking response of free-standing rigid blocks, which is characterised by the alternation of impacts between the block and the foundation that suddenly change the contact point between the two members. Nonlinear dynamic analysis with implicit time integration is carried out to study rocking initiation (uplift) and rocking attenuation (at impact) of free-standing rigid blocks with different slenderness under pulse-type motions. The attenuation effects are further studied by allowing the block to rock freely on the foundation. Solid homogenous sections are analysed with fully integrated 4-node plane stress quadrilateral elements (CPS4) for the block and the equivalent reduced integration elements (CPS4R) for the foundation. Rigid body constraints are used to refer the motion of each body to the respective centre of gravity. Contact is treated using the small-sliding formulation and the resulting system of equations of dynamics is solved by means of the Abaqus/Standard HHT algorithm, with the value of alpha that provides the maximum numerical dissipation. A sensitivity analysis is conducted for the time incrementation and mesh element size. Large time steps lead to higher attenuation of rocking movement due to the increment of the contact constraint discontinuity work (ALLCCDW), an energy component which highly influences rocking movement. However, smaller values of the step time yield very accurate results in comparison with the analytical solution. The element size sensitivity analysis revealed that the rocking initiation is generally well captured, but the coarse mesh results in inaccurate capture of the instant at which impact occurs and unrealistic attenuation of the rocking response. On the contrary, the fine mesh (defined as 1% of the corresponding contact surface) seems to capture well the rigid rocking response. These suggest that the selection of the analysis parameters is crucial to capture the desired response of free-standing rigid blocks.

Keywords: Rocking; Rigid block; Finite element modelling; Contact formulation; Impact; Abaqus Implicit

1. Introduction

1. The rocking response of free-standing rigid blocks on rigid foundation under seismic excitation has been studied for more than a century (Milne, J., "Seismic Experiments," *Trans. Seismol. Soc. Jpn.*, 8, 1-82, 1885.). The beneficial isolation effects of rocking for the structures have been widely observed, making it a useful design approach to reduce damage of vertical elements. Housner (Housner, G. W., "The Behavior of Inverted Pendulum Structures during Earthquakes," *Bulletin of the Seismological Society of America*, 53(2), pp. 403-417, 1963.) introduced the basic equations of motion of free-standing rigid blocks, and

- paved the way for a number of more recent studies on this topic (Makris, N., Y.S. Roussos, "Rocking Response of Rigid Blocks under Near-Source Ground Motions," *Geotechnique*, 50(3): 243-262, 2000., Ozer, M., F. Alisverisci, "Dynamic Response Analysis of Rocking Rigid Blocks subjected to Half-Sine Pulse type Base Excitations," *Vibration Problems ICOVP 2005*, 389-394, 2007 Springer, 2007.
2. Roussis, P.C., S. Odysseos, "Overturning of a Free-Standing Block to a Full-Cycle Seismic Pulse," *Proc.*, 15th World Conf. on Earthquake Engineering, Lisboa, 2012.
 3. Vassiliou, M. F., B. Stojadinovic, K. R. Mackie, "A Finite Element Model for Seismic Response Analysis of Deformable Rocking Frames," *Earthquake Engng Struct. Dyn.*, 2016.
- Zhang, J., N. Makris, "Rocking Response of Free-Standing Blocks under Cycloidal Pulses," *J. Eng. Mech.*, 2001, 127(5): 473-483, 2001., Ozer, M., F. Alisverisci, "Dynamic Response Analysis of Rocking Rigid Blocks subjected to Half-Sine Pulse type Base Excitations," *Vibration Problems ICOVP 2005*, 389-394, 2007 Springer, 2007., Makris, N., M. F. Vassiliou, "Sizing the Slenderness of Free-Standing Rocking Columns to Withstand Earthquake Shaking," *Arch Appl Mech*, 82:1497-1511, 2012., Dimitrakopoulos, E. G., M.J. DeJong, "Revisiting the Rocking Block: Closed-form Solutions and Similarity laws." *Proc. R. Soc. A*, 468, 2294-2318, 2012., Roussis, P.C., S. Odysseos, "Overturning of a Free-Standing Block to a Full-Cycle Seismic Pulse," *Proc.*, 15th World Conf. on Earthquake Engineering, Lisboa, 2012., Vassiliou, M. F., B. Stojadinovic, K. R. Mackie, "A Finite Element Model for Seismic Response Analysis of Deformable Rocking Frames," *Earthquake Engng Struct. Dyn.*, 2016., Kalliontzis, D., S. Sritharan, A. E. Schultz, "Improving Accuracy of the Simple Rocking Model of Rigid Blocks," *Proc. 16th World Conf. on Earthquake Engineering*, Santiago, Paper No. 451, 2017.). The key factor that governs attenuation of rocking response is the coefficient of restitution, a constant that depends on the slenderness of the rocking block and attenuates its response during impact.

Abaqus (Abaqus 6.14-1, "Analysis User's Manual") provides a broad range of contact interaction properties for elastic and rigid bodies. However, rocking is usually studied numerically with special-purpose software packages based on the Distinct Element Method, rather than general-purpose Finite Element software packages such as Abaqus. The suitability of the explicit analysis in impact-related problems is well-known, however the analysis presented herein considers only rigid elements, for which implicit dynamic analysis is recommended.

In the ideal case of a rigid block on a rigid foundation, the only damping mechanism directly related to the rocking response of a rigid block is introduced by its impact against the surface where it rests. This impact introduces an instantaneous and discontinuous energy dissipation mechanism. The Abaqus Implicit solver does not allow to define the coefficient of restitution which in the analytical solution is used to quantify damping. Introducing an equivalent viscous damping to simulate this dissipation in the Implicit analysis seems inappropriate given the discontinuous nature of the actual damping during rocking.

A procedure using Abaqus to model and quantify the in-plane rocking response of free-standing rigid blocks is presented herein. Two types of sensitivity analysis are conducted in order to optimise the numerical response: time-step, and mesh sensitivity. It is observed that long time-steps increase significantly the so-called "discontinuity work", a non-physical energy component that accounts for the portion of the work done by contact forces that is not accounted for by other contact energy variables (Abaqus 6.14-1, "Analysis User's Manual"). Hence, smaller time-step increments are required for accurately capturing the rocking response of rigid blocks. In terms of

the mesh size, smaller elements yield more accurate results by capturing time instant which impact occurs and attenuating rocking movement with high accuracy compared to the analytical solution.

2. Analytical solution

- The analytical solution (as opposed to the numerical, finite element, one) is formulated for the block presented in Figure 1, with height and width $2h$ and $2b$, respectively. The block can oscillate around the centres of rotation O and O' when it is set to rocking. Its centre of gravity coincides with the geometric centre located at a distance R from any corner. The rest angle, or slenderness α , is given by $\tan(\alpha) = b/h$. Depending on the value of the ground acceleration and the coefficient of friction (between the block and the foundation), μ , the block may translate with the ground, enter in a rocking motion, or slide. A necessary condition for the block to start rocking is $\mu > b/h$, (Abaqus 6.14-1, "Analysis User's Manual")

Aslam, M., W. G. Godden, and D. T. Scalise, "Earthquake Rocking Response of Rigid Bodies," (1978). In this study it is assumed that μ is sufficiently large to prevent sliding at any instant. Under a negative horizontal ground acceleration, \ddot{u}_g , the block will initially rotate around the pivot point O with a positive rotation, $\theta > 0$ (clockwise rotation), and if it does not overturn, it will eventually have a negative rotation, and so forth. The dynamic moment equilibrium about the pivot points gives the equations of motion for the rocking of free-standing rigid blocks:

$$-m \cdot \ddot{u}_g(t) \cdot R \cdot \cos[\pm a - \theta(t)] = I_O \cdot \ddot{\theta}(t) + m \cdot g \cdot R \cdot \sin[\pm a - \theta(t)] \quad (1)$$

In this expression, and whenever there is a double sign (say \pm), the top positive sign is for $\theta(t) > 0$, and the bottom negative sign is for $\theta(t) < 0$.

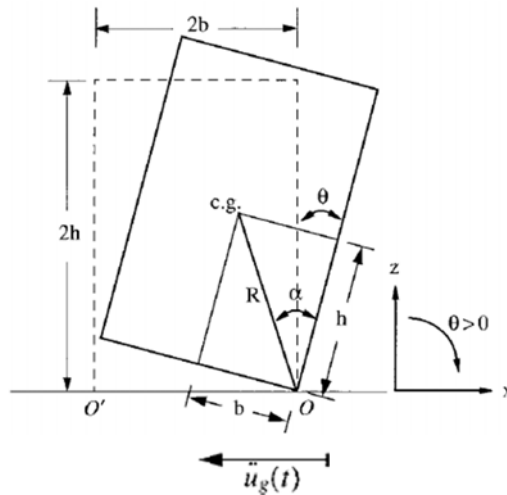


Figure 1. Free-standing rigid block.

The solution of Equation (1) yields the angular acceleration of the free-standing block:

$$\ddot{\theta}(t) = -p^2 \left\{ \sin[\pm\alpha - \theta(t)] + \frac{\ddot{u}_g}{g} \cos[\pm\alpha - \theta(t)] \right\} \quad (2)$$

Equations (1) and (2) are valid for arbitrary values of the slenderness α . For tall and slender blocks α is relatively small and the previous expressions can be linearised. Assuming also that the ground acceleration is sinusoidal, Equation (2) can be simplified to:

$$\ddot{\theta}(t) = -p^2 \cdot \frac{ap}{g} \sin(\omega_p t + \psi) + p^2 \cdot \theta(t) \mp p^2 \cdot a \quad (3)$$

where $\psi = \sin^{-1}(\alpha \cdot g / a_p)$ is the phase delay due to initiation of rocking.

By integrating Equation (3), the angular velocity and rotation of the rigid block can be obtained as:

$$\dot{\theta}(t) = p \cdot A_{3/1} \cdot \cosh(pt) + p \cdot A_{4/2} \cdot \sinh(pt) + \frac{\omega_p}{1 + (\omega_p/p)^2} \frac{ap}{g} \cos(\omega_p t + \psi) \quad (4)$$

$$\theta(t) = A_{3/1} \cdot \sinh(pt) + A_{4/2} \cdot \cosh(pt) \pm a + \frac{1}{1 + (\omega_p/p)^2} \frac{ap}{g} \sin(\omega_p t + \psi) \quad (5)$$

where:

$$A_1 = A_3 = \frac{\dot{\theta}_o}{p} - a \frac{\omega_p/p}{1 + \omega_p^2/p^2} \frac{\cos(\psi)}{\sin(\psi)} \quad (6)$$

$$A_2 = \theta_o + \alpha - \frac{\alpha}{1 + \omega_p^2/p^2} \quad (7) \quad A_4 = \theta_o - \alpha - \frac{\alpha}{1 + \omega_p^2/p^2} \quad (8)$$

Referring the rigid body motion to the centre of gravity (CG) of the block movement, the horizontal (x) and the vertical (y) displacement and velocity can be obtained:

$$\begin{aligned} u_x^{CG}(t) &= \pm R \cdot (\sin a - \sin[a \mp \theta(t)]) \\ u_y^{CG}(t) &= R \cdot (\cos[a \mp \theta(t)] - \cos a) \\ v_x^{CG}(t) &= R \cdot \cos[a \mp \theta(t)] \cdot \dot{\theta}(t) \\ v_y^{CG}(t) &= \pm R \cdot \sin[a \mp \theta(t)] \cdot \dot{\theta}(t) \end{aligned} \quad (9)$$

The dissipation of the rocking movement after each impact is analytically described by the coefficient of restitution, η , which is defined as the ratio between the angular velocity just after, and just before, the impact ($\dot{\theta}^+$ and $\dot{\theta}^-$, respectively). Based on the conservation of momentum about the pivot points, the coefficient of restitution can be expressed as a function of the slenderness α :

$$\eta = \left[1 - \frac{3}{2} \sin^2(a) \right] \quad (10)$$

3. Proposed modelling procedure

3.1 Rocking Body

The rigid body motion is enforced here with a body-constraint applied to the deformable bodies. The centre of gravity of each body is used as the reference point in this constraint formulation to relate the movement of the corresponding body to the movement of its reference point.

The block and the foundation are modelled using planar shell elements and meshed by 4-node bilinear plane stress continuum elements. The elements in the block have full integration (CPS4) and the elements in the foundation have reduced integration with hourglass control (CPS4R). It has been observed that using full integration continuum elements (CPS4) in the foundation gives very similar results.

A homogeneous elastic material with Young's modulus and Poisson's ratio equal to 30GPa and 0.20, respectively, is assigned to the block and the foundation. The mass and rotary inertia of the rigid bodies, the only restoring mechanisms in the rocking response, are defined through the density of the material. Although this is a distributed mass definition, the rigid body constraint formulation gathers the total mass of the block at the defined reference point and simplifies the rotary inertia to the value $I = \Sigma(mR^2) = 4mR^2 / 3$. However, it has been verified that the value of this density has no influence on the rocking response of free-standing blocks in Abaqus, which is consistent with the analytical solution (see Equations (2), (3), (4), (5)). Hence, the mass density is set equal to 2,500kg/m³ (=2.5tn/m³).

In total, four different blocks with different slenderness are examined. The geometry of these blocks is shown in Table 1.

Table 1. Block parameters.

No. block	Height $2h$ (m)	Width $2b$ (m)	Slenderness a (rad)	Coefficient of restitution η
1	1.20	0.40	0.322	0.850
2	1.20	0.30	0.245	0.912
3	2.00	0.40	0.197	0.942
4	2.00	0.20	0.100	0.985

3.2 Rocking surface

A contact pair between the block and the foundation is used to define the interaction between them. Although the advantages of surface-to-surface contact are well documented, due to the nature of this problem wherein the rigid block can tilt standing only at the pivot point, a node-to-surface contact discretization is selected between the two pivot points and the foundation surface. A small sliding formulation is selected due to the reduced relative movement of the two interacting rigid bodies.

A "hard" contact pressure-overclosure relationship is used to prevent penetration of the pivot points in the foundation (master) surface. Separation of the two contact members is allowed with the augmented Lagrange method in order to facilitate the solution of the contact problem. Sliding is assumed to be prevented during the analysis between the contact bodies, hence "rough" friction is used offering an infinite coefficient of friction.

3.3 Analysis process

An implicit direct-integration dynamic analysis with fixed time increment is implemented. Although automatic incrementation is recommended for general-purpose analyses because it allows to reduce/increase the time increment according to the needs of the analysis, fixed time incrementation is selected to keep the discontinuity work within admissible values. The same numerical model was run with different increment definition, e.g. with fixed time incrementation 10^{-3} s and with automatic incrementation using maximum time-step equal to 10^{-3} s, showing that the strict fixed time incrementation yields more accurate results as shown in Figure 2.

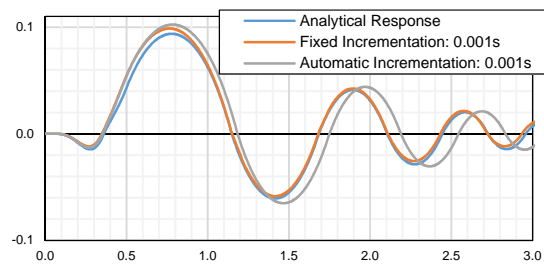


Figure 2. Comparison of fixed with automatic incrementation.

The implicit HHT algorithm (Hilber, H. M., T. J. Hughes, R. L. Taylor, “Improved Numerical Dissipation for Time Integration Algorithms in Structural Dynamics,” *Earthquake Engineering & Structural Dynamics*, 5(3):283–292, 1977.) is selected to integrate the system of equations of dynamics. The numerical damping introduced by the HHT in the high-order vibration is controlled by the parameter α_{HHT} , which assumes values between -0.50 and 0.00. This parameter was expected to be important in the dynamic response given the alternation of impacts that characterise rocking. However, it was observed that for the case of a relative small time increment value (10^{-3} s) combined with relatively small element size (1% of corresponding contact surface), the value of α_{HHT} does not affect significantly the response. In all subsequent analyses α_{HHT} is set equal to -0.333, which provides the maximum numerical dissipation (Hilber, H. M., T. J. Hughes, R. L. Taylor, “Improved Numerical Dissipation for Time Integration Algorithms in Structural Dynamics,” *Earthquake Engineering & Structural Dynamics*, 5(3):283–292, 1977.).

It should be noted that the only damping source which was modelled is numerical damping in the HHT algorithm. No other damping models were utilised. However, it will be shown that independently of the analysis parameters, Abaqus attenuates rocking movement after each impact by decreasing the velocity field. The results show close agreement with the analytical solution for the case of sufficiently small values for the time-step and the mesh size.

The dynamic analysis starts with a free rocking study in which the initial rotation (tilt) shown in Table 2 is applied to the blocks as can be seen in Figure 3. The objective of this initial analysis is to examine the rocking attenuation through the sequence of impacts. The next analysis is a

base-induced rocking case, wherein the sinusoidal acceleration pulses included in Table 2 are applied to the foundation surface in order to examine how the movement is transferred to the block and rocking is initiated and then damped through the free rocking response of the block.

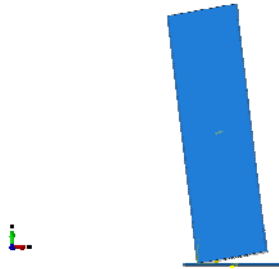


Figure 3. Free rocking response of free-standing rigid block.

Table 2. Free and base-induced rocking parameters.

No. block	Free rocking	Base-induced rocking		
	Initial Rotation θ_0 (rad)	Amplitude a_p (g)	Duration T_p (sec)	Angular frequency ω_p (rad/sec)
1	0.15	0.55	0.50	12.566
2	0.15	0.40	0.50	12.566
3	0.07	0.30	0.50	12.566
4	0.07	0.15	0.50	12.566

4. Discussion of the results

This Section presents the comparison between the analytical solution of the expressions presented in Section 2 and the numerical results obtained with the Implicit dynamic analysis in Abaqus.

4.1 Free rocking

The value of the time-step was found critical for the accuracy of the numerical models compared to the analytical solution while it determines the value of an energy component related to contact interaction which highly influences the accuracy of the results. An energy balance examination is conducted which reveals that this influence is highly negative and leads to inaccurate attenuation of rocking movement.

4.1.1 Influence of the time-step

Three different values for the fixed time increment value (10^{-3} s, $5 \cdot 10^{-3}$ s and $10 \cdot 10^{-3}$ s) are examined here. The element size is kept constant and uniform in the entire block, with square elements of length equals to 1% of the corresponding contact surface. The free rocking responses for Blocks 1, 2 are presented in Figures 4a and 4b, respectively. Confirming the analytical solution, in which larger blocks attenuate rocking movement faster, the response of Block 1 shows smaller rocking cycles and it returns to the equilibrium earlier than Block 2. Nevertheless, numerical models appear differences dependent on the time-step value. Larger time increment values lead to faster attenuation of the rocking response compared to the analytical solution, which consequently leads to a significant time delay in the rocking motion

after the first cycles of movement. However, the smallest time-step (10^{-3} s) yields very accurate results and the response is almost superimposed with the analytical one. The numerical result captures the attenuation of the rocking movement correctly, although a small time lag occurs for Block 2 by the end of the response ($t > 2.6$ s). Interestingly, in all the acceleration responses obtained from the numerical models some degree of noise appears, related to a high-order vibration, which is not observed in the analytical result.

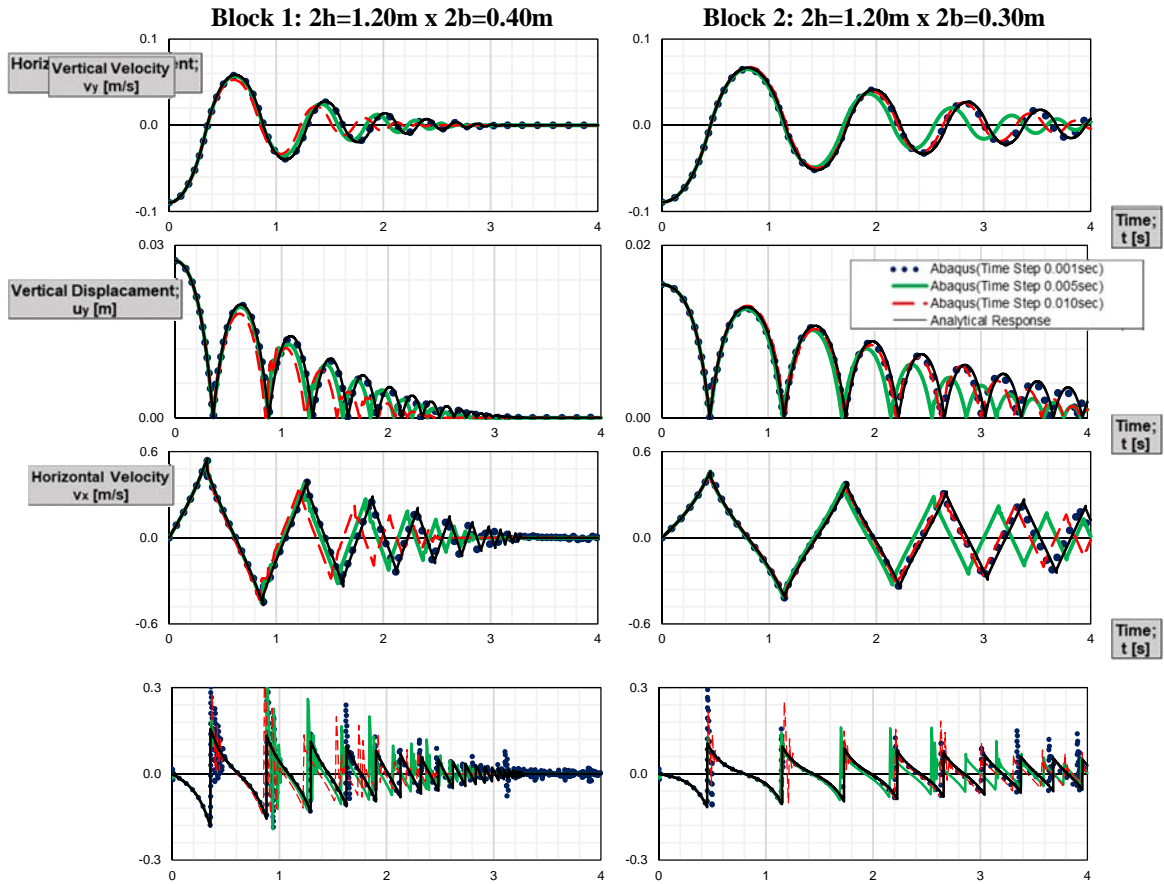


Figure 4. Influence of the time-step on the free rocking response of: (a) Block 1; (b) Block 2.

The high influence of time increment size is explained by examining the energy balance of the rocking system:

$$E_{TOTAL} = E_{KE} - E_W - E_{CW} \quad (10)$$

where the total energy of the rocking system (E_{TOTAL}) equals to the kinetic energy (E_{KE}) of the block subtracting the external work (E_W) which is the sum of the stored and part of the

dissipated energy due to contact forces. The fourth energy component introduced in the energy balance presented by Equation (10) is E_{CW} , an energy variable associated with contact constraint “discontinuity work” which accounts for the portion of the work done by contact forces which cannot be accounted for by other contact energy variables. Although according to the Abaqus documentation (Abaqus 6.14-1, “Analysis User’s Manual”) E_{CW} can have a significant value without introducing relevant inaccuracies, in this specific case it is very influential and the errors introduced can make the rocking response very inaccurate, as will be shown in the following.

The energy balance in the free rocking response of Block 1 with 10^{-3} s and $10 \cdot 10^{-3}$ s time-steps, presented in Figures 5a and 5b, respectively. The external work appears to peak at each impact of the block. The kinetic energy also peaks at those instances but it reduces its value gradually as it depends on the velocity of the block and this is attenuated. Each impact also affects the “discontinuity work” and the total energy, which are almost constant between those instants. The large difference in terms of the “discontinuity work” for these models reveals the high influence of this energy component on rocking response. The smaller time increment, which leads to an accurate rocking response, keeps E_{CW} relatively low compared to the other energy sources. This is due to the time intervals at which the contact forces after and before impact are calculated are very close to each other and the “discontinuity work” is reduced. On the other hand, E_{CW} is significantly large when the time-step is $10 \cdot 10^{-3}$ s leading to faster attenuation of rocking movement.

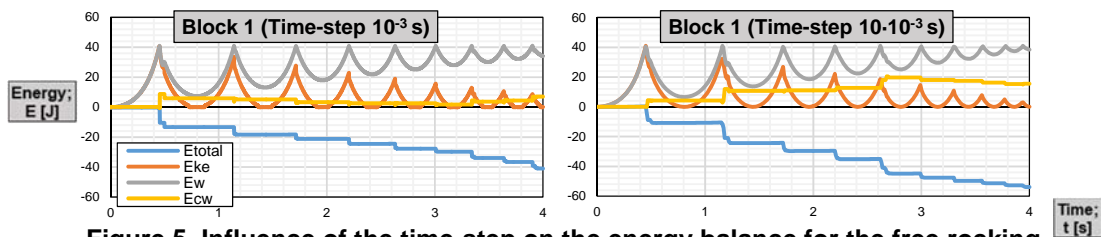


Figure 5. Influence of the time-step on the energy balance for the free rocking response of Block 1: (a) 10^{-3} s; (b) $10 \cdot 10^{-3}$ s.

The same trend of faster attenuation for Block 3, a geometrically larger block compared to Block 4, has been observed in the response included in Figures 6a and 6b. Again, the larger time-step increment values attenuate rocking movement faster, in contrast to the 10^{-3} s time increment which yields a very accurate result and is able to represent the attenuation of the rocking movement correctly. However, a considerable time delay occurs in these numerical models for both blocks by the end of the response ($t > 2.5$ s). The noise that appeared in the vertical linear variables of the response is also present in these models, revealing the existence of high-order vibration components.

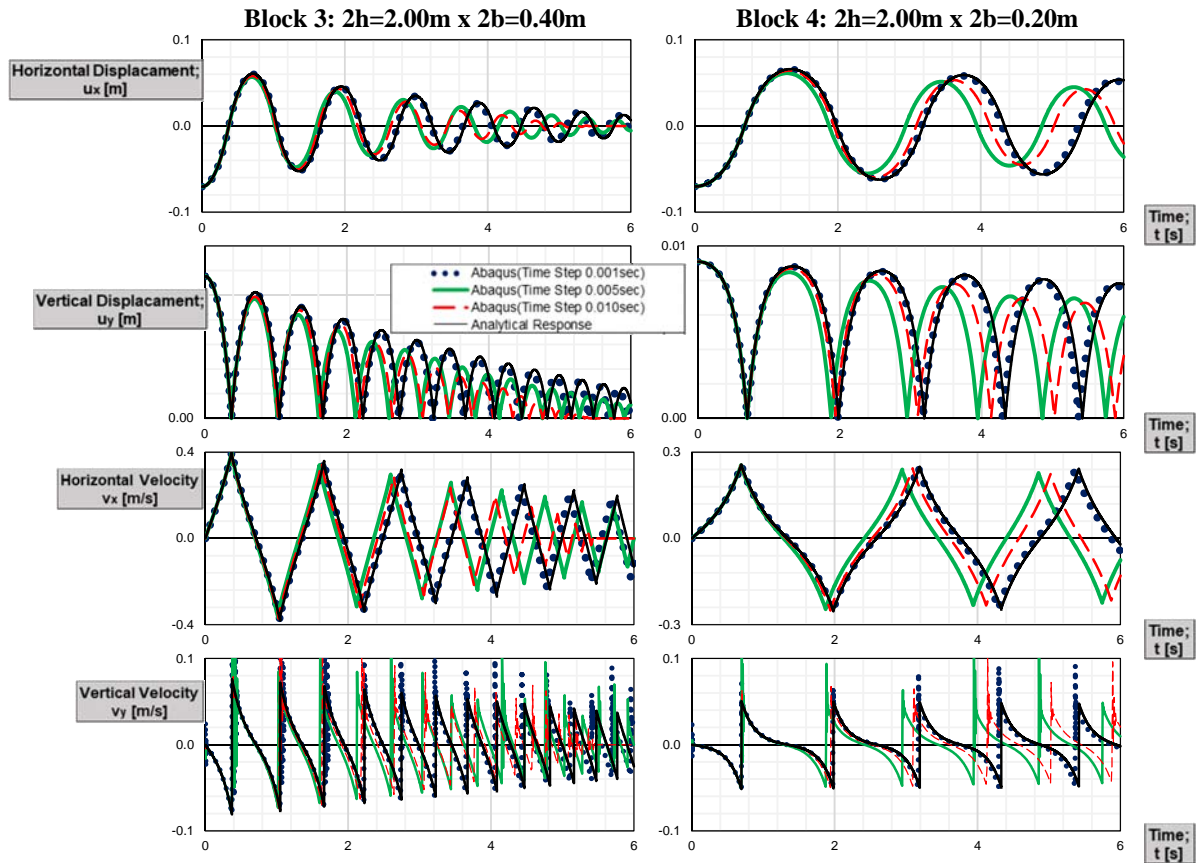


Figure 6. Influence of the time-step on the free rocking response of: (a) Block 3; (b) Block 4.

The high influence of contact constraint “discontinuity work” is confirmed for both blocks. Again, the smallest time increment value results in a more accurate energy dissipation. Hence, it can be concluded that E_{cw} has a significant influence on the accuracy of the rocking response of free-standing rigid blocks.

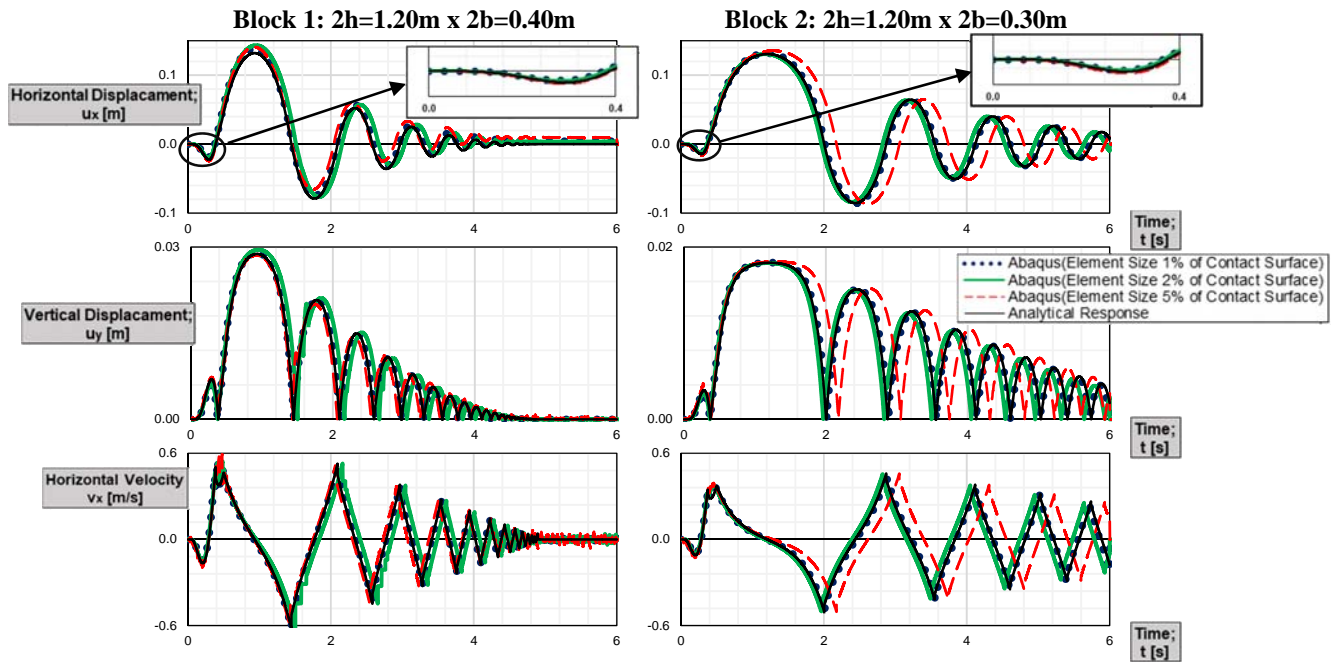
4.2 Base-induced rocking

In this case a sinusoidal movement is imposed on the foundation surface according to Table 2 that idealises an earthquake. The rocking response is analysed for different mesh sizes in order to establish the appropriate mesh size for the problem studied. Ultimate goal of this section is to examine transfer of movement to the block and attenuation dependent on the element size.

4.2.1 Influence of the mesh size

Three different values for the element size have been considered, namely 1%, 2% and 5% of the corresponding contact surface. The time-step in this case is kept constant and equal to 10^{-3}

s, which renders the most accurate solution as it was observed previously. The rocking responses of Blocks 1 and 2 under a sinusoidal pulse are presented in Figures 7a and 7b, respectively. The models, regardless of the element size, capture very accurately the uplift of the block during the excitation and the subsequent attenuation of the rocking movement, because this is influenced by the size of the time-steps in the analysis and it is kept to a very low value in all cases (10^{-3} s). The displacements in all models during the base motion is very similar. However, after this stage the model for Block 2 with the coarsest mesh (5% of the base length) presents a significantly longer first rocking cycle and this introduces a time-delay in the response that is carried over in the rest of the rocking motion. It is also observed that the model with the largest size element in Block1 introduces permanent horizontal displacement, which is not consistent with the “rough” friction definition used in the modelling procedure. In terms of velocity, the coarser mesh introduces a significant noise in the response that is not present in the model with the finest mesh, which captures accurately the rocking response.



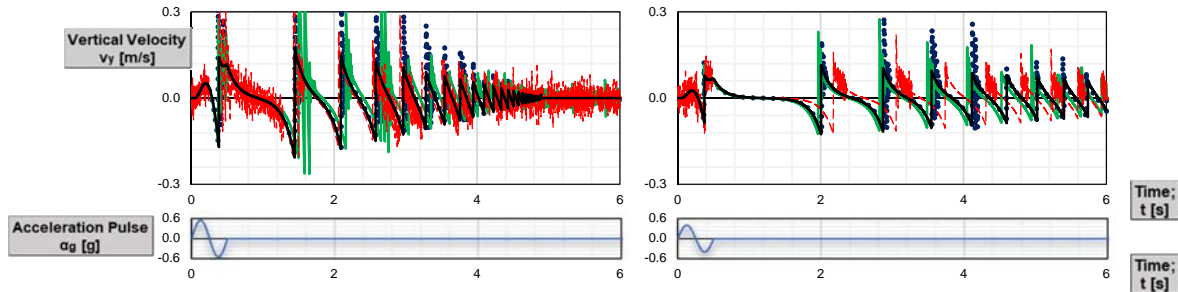


Figure 7. Influence of the mesh size on the rocking response induced by the movement of the base. (a) Block 1; (b) Block 2.

Although a damping source is not specifically introduced in the model, apart from the high-order numerical damping in the HHT solver, Abaqus attenuates the rocking movement by decreasing angular velocity at each impact. It has been confirmed (by carrying out a sensitivity analysis for alpha) that this is not due to the HHT damping. Table 3 presents the equivalent coefficient of restitution for every model and the corresponding time instant of the impact. The former is calculated by the traditional definition of coefficient of restitution, e.g. by dividing the velocity just after impact with the one just before it, while the latter by a linear interpolation due to the fixed time incrementation as in some cases the exact instant at which impact occurs is not captured.

It can be seen that the time instants of impact are well captured, especially by the model with the finer mesh, whereas the error introduced by the coarser mesh is clear from this table. Although the models with finer mesh seem to capture the analytical response sufficiently well, as shown in Figures 7a and 7b, the attenuation of rocking movement is introduced by equivalent restitution coefficients that are not constant across impacts, unlike in the analytical solution. The numerical solver seems to be adjusting the velocity fields after the impacts to obtain the correct response.

Table 3. Coefficients of restitution at different impacts for the Blocks 1 and 2. The error (given in parentheses) is with respect to the analytical solution.

		Block 1: 2h=1.20m x 2b=0.40m				Block 2: 2h=1.20m x 2b=0.30m			
		Analytical Solution	Model 1: 1% of Con. Surf.	Model 2: 2% of Con. Surf.	Model 3: 5% of Con. Surf.	Analytical Solution	Model 1: 1% of Con. Surf.	Model 2: 2% of Con. Surf.	Model 3: 5% of Con. Surf.
2 nd Impact	Time instant (sec)	1.447	1.450 (0.21%)	1.503 (3.87%)	1.431 (-1.11%)	2.005	2.012 (0.35%)	1.964 (-2.04%)	2.176 (8.53%)
	Coefficient of restitution	0.850	0.911 (7.18%)	0.736 (-13.41%)	0.780 (-8.24%)	0.912	0.884 (-3.07%)	0.911 (-0.11%)	0.899 (-1.43%)
6 th Impact	Time incident (sec)	3.283	3.285 (0.06%)	3.357 (2.25%)	3.227 (-1.71%)	4.605	4.600 (-0.11%)	4.530 (-1.63%)	4.800 (4.23%)
	Coefficient of restitution	0.850	0.735 (-13.53%)	0.807 (-5.06%)	0.902 (6.12%)	0.912	0.917 (0.55%)	0.906 (-0.66%)	0.907 (-0.55%)
9 th Impact	Time incident (sec)	3.945	3.944 (-0.03%)	4.010 (1.65%)	3.934 (-0.28%)	5.739	5.715 (-0.42%)	5.641 (-1.71%)	5.929 (3.31%)
	Coefficient of restitution	0.850	0.757 (-10.94%)	0.881 (3.65%)	0.908 (6.82%)	0.912	0.931 (2.08%)	0.877 (-3.84%)	0.902 (-1.10%)

A considerable difference in the numerical coefficients of restitution with respect to the analytical model is observed, especially for Block 1. A further examination of results from the most accurate numerical models is conducted and a comparison with the constant coefficient of restitution of the analytical solution is made for every impact in Figures 8a and 8b. Abaqus attenuates the rocking movement with a numerical coefficient of restitution that is in most cases lower than the analytically predicted constant value. The average difference for Block 2 is negligible (only -1.45%), while the corresponding difference for Block 1 has a higher value (-4.94%). However, it must be highlighted that the most relevant impacts are those occurring at the beginning of the response because they introduce a larger damping into the movement. Hence, the first four impacts for Block1 lead to an equivalent numerical coefficient of restitution equal to 0.849 which is only 0.01% lower than the analytically predicted value.

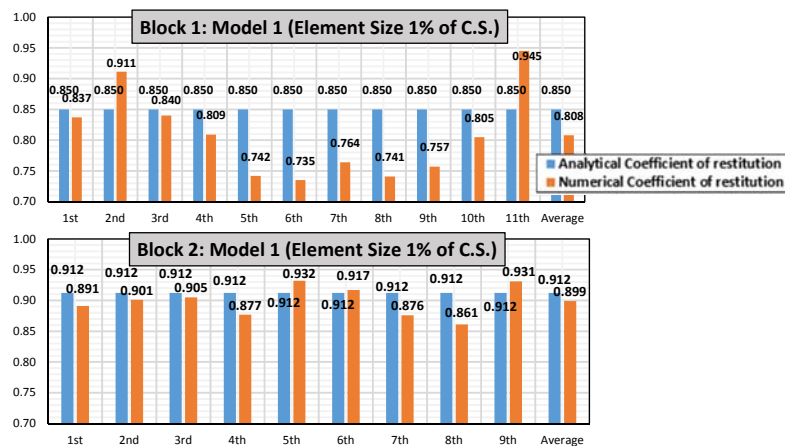


Figure 8. Numerical coefficients of restitution for models with mesh size 1% of contact surface and time-step 10^{-3} s. Comparison with the analytical value. (a) Block 1; (b) Block 2.

The rocking response of Blocks 3 and 4 under a sinusoidal pulse is presented in Figures 9a and 9b, respectively. Contrary to the results shown in Figures 7a and 7b, coarser mesh models do not capture accurately the uplift (rocking initiation) of the block during the excitation. This inaccuracy leads to a longer first rocking cycle, which is carried over the rest of the response with quite accurate attenuation at the impacts, as can be seen from successive peak values. Again, the finest mesh model yields the most accurate results for both blocks. Lack of noise in these models reveals that the influence of high-order vibration modes is negligible determining the fine mesh (1%) as the most accurate numerical approach.

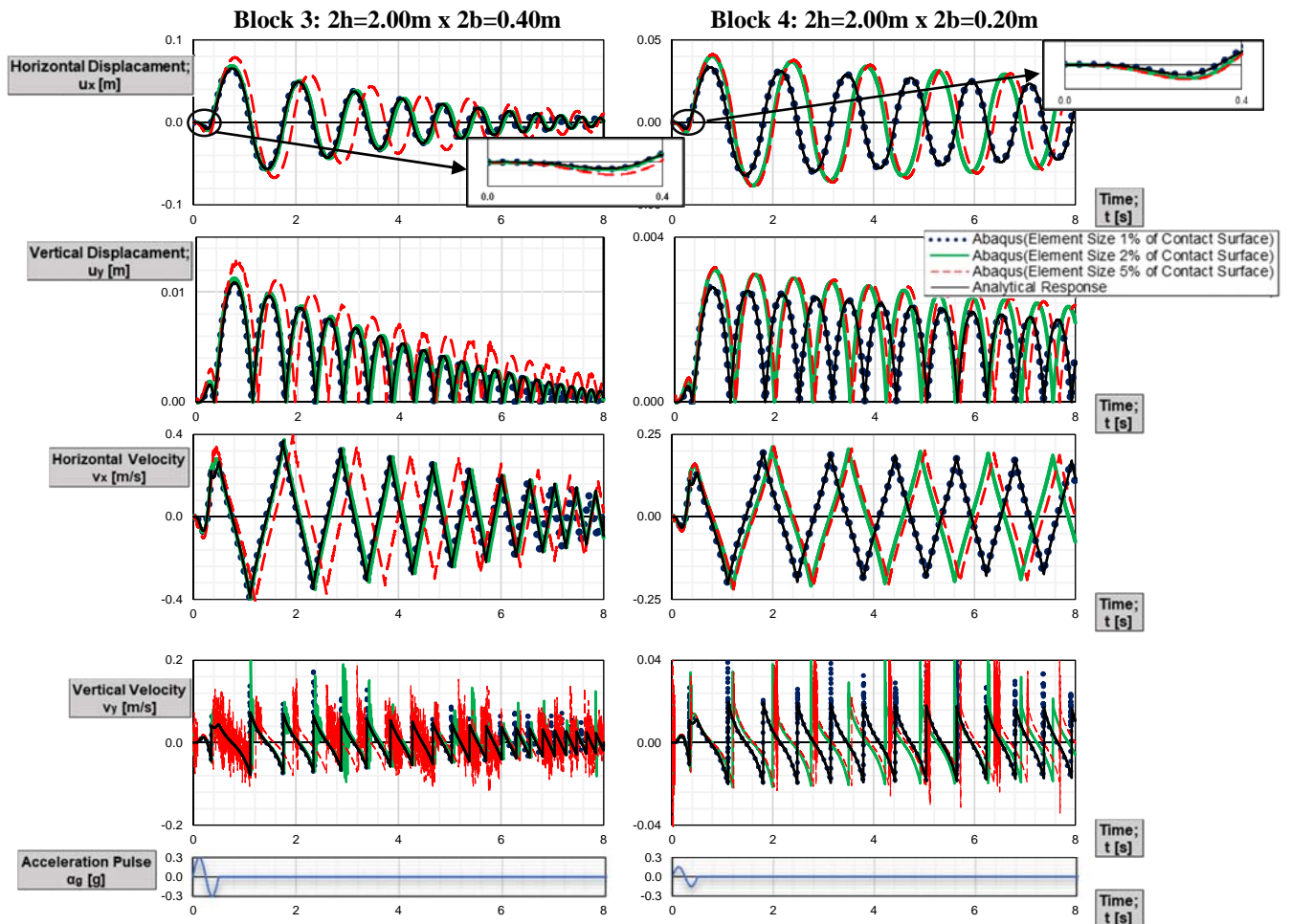


Figure 9. Influence of mesh size on the rocking response induced by the movement of the base. (a) Block 3; (b) Block 4.

Time of impact and equivalent numerical coefficients of restitution calculated from the numerical models are presented in Table 4. Confirming the results presented in Figures 9a and 9b, the smallest size element models capture time of impact with high accuracy contrary to larger size element models which seem to miss it. Furthermore, fine mesh models seem to attenuate rocking movement with high accuracy since the difference between numerical and analytical coefficients of restitution is minimal.

Table 4. Coefficients of restitution at different impacts for Blocks 3 and 4. The error (given in parentheses) is with respect to the analytical solution.

		Block 3: 2h=2.00m x 2b=0.40m				Block 4: 2h=2.00m x 2b=0.20m			
		Analytical Solution	Model 1: 1% of Con. Surf.	Model 2: 2% of Con. Surf.	Model 3: 5% of Con. Surf.	Analytical Solution	Model 1: 1% of Con. Surf.	Model 2: 2% of Con. Surf.	Model 3: 5% of Con. Surf.
3 rd Impact	Time instant (sec)	1.756	1.748 (-0.46%)	1.775 (1.08%)	1.941 (10.54%)	1.808	1.804 (-0.22%)	1.993 (10.23%)	2.025 (12.00%)
	Coefficient of restitution	0.942	0.948 (0.64%)	0.947 (0.53%)	0.920 (-2.34%)	0.985	0.981 (-0.41%)	0.976 (-0.91%)	0.981 (-0.41%)
6 th Impact	Time instant (sec)	3.382	3.382 (0.00%)	3.429 (1.39%)	3.737 (10.50%)	3.795	3.795 (0.00%)	4.227 (11.38%)	4.295 (13.18%)
	Coefficient of restitution	0.942	0.976 (3.61%)	0.906 (-3.82%)	0.963 (2.23%)	0.985	0.976 (-0.91%)	0.980 (-0.51%)	1.004 (1.93%)
9 th Impact	Time instant (sec)	4.670	4.661 (-0.19%)	4.720 (1.07%)	5.170 (10.71%)	5.645	5.640 (-0.09%)	6.271 (11.09%)	6.384 (13.09%)
	Coefficient of restitution	0.942	0.939 (-0.32%)	0.912 (-3.18%)	0.894 (-5.10%)	0.985	0.970 (-1.52%)	0.968 (-1.73%)	0.979 (-0.61%)

Figures 10a and 10b present the equivalent coefficients of restitution for Blocks 3 and 4, respectively. The difference in the distinct impacts is minimal for both blocks leading to an average difference of -1.49% for Block 3 and -0.82% for Block 4 which is negligible in both cases. Hence, Abaqus attenuates rocking movement quite accurately for slender blocks ($\eta \geq 0.90$) such as Blocks 2, 3 and 4. Consequently, it is noted that no trend is found for the equivalent coefficient of restitution since its value can be either smaller or larger than the constant value used in the analytical solution, independently of the number of impacts and the type of the block.

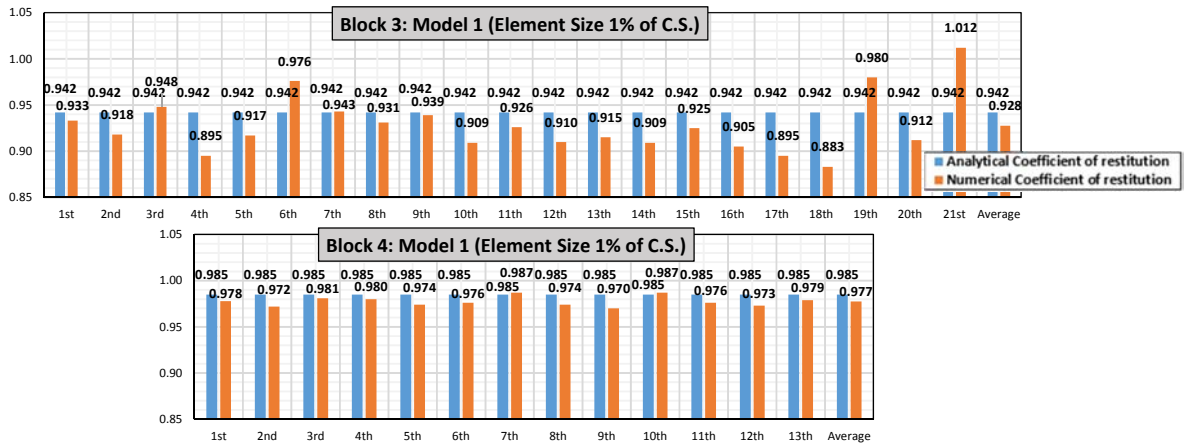


Figure 10. Numerical coefficients of restitution for models with mesh size 1% of contact surface and time-step 1E-3s. Comparison with the analytical value. (a) Block 3; (b) Block 4.

5. Conclusions

Abaqus/Standard has been used herein to model the in-plane rocking response of rigid blocks with different slenderness under free and base-induced vibration conditions. The model defines a node-to-surface contact at the base-foundation surface and the equations of dynamics are solved with the implicit HHT algorithm.

It has been observed that the time-step has a large influence on the free rocking movement. High values of this parameter introduce a significant “discontinuity work” that leads to inaccurate responses history in terms of displacements, and, especially, velocities. However, a fixed time-step of 10^{-3} s reduces the discontinuity work to admissible levels and yields accurate responses in the different blocks.

The influence of the mesh size was studied in the block models under pulse-like base excitations. It was observed that the rocking initiation is well captured for Blocks 1 and 2, unlike Blocks 3 and 4 wherein fine mesh (1% of corresponding contact surface) is demanded to obtain accurate initiation of uplift, revealing no trend for this type of block (squat or slender). These numerical models are the only ones that are able to capture the instants at which each impact occurs, avoiding a significant noise in the velocity of the block.

Although no coefficient of restitution is introduced by the user in Abaqus, the Implicit solver is able to represent the dissipation during rocking. The equivalent coefficient of restitution is calculated from the response history in Abaqus and it was observed that although this coefficient is not constant during the analysis, the response matches the analytical solution satisfactorily. Abaqus seems to relate the slenderness of the block to the attenuation at each impact. This is confirmed by the low values of equivalent coefficients of restitution presented in Table 4 which are lower for less slender blocks, consistently with the analytical solution. In terms of maximum values, for Blocks 1 and 3 extreme value of 0.945 and 1.012, respectively, are recorded, with the second larger being equal to 0.911 and 0.980.

Table 5. Range of values of equivalent coefficient of restitution and comparison with the analytical solution.

Block 1: 2h=1.20m x 2b=0.40m		Block 2: 2h=1.20m x 2b=0.30m		Block 3: 2h=2.00m x 2b=0.40m		Block 4: 2h=2.00m x 2b=0.20m	
Analytical Solution	Model 1: 1% of Con. Surf.	Analytical Solution	Model 1: 1% of Con. Surf.	Analytical Solution	Model 1: 1% of Con. Surf.	Analytical Solution	Model 1: 1% of Con. Surf.
0.850	0.735 – 0.945 (av. 0.808)	0.912	0.861 – 0.932 (av. 0.899)	0.942	0.883 – 1.012 (av. 0.928)	0.985	0.970 – 0.987 (av. 0.977)

In conclusion, although a direct definition of coefficient of restitution is currently not possible in Abaqus, numerical models with the appropriate time-step and mesh size accurately capture the response of free-standing rigid blocks. Nonetheless, a direct definition of coefficient of restitution would improve the potential of Abaqus in this type of analysis, hence would be a welcome addition in future versions.

References

5. Abaqus 6.14-1, "Analysis User's Manual"
6. Aslam, M., W. G. Godden, and D. T. Scalise, "Earthquake Rocking Response of Rigid Bodies," 1978.
7. Dimitrakopoulos, E. G., M.J. DeJong, "Revisiting the Rocking Block: Closed-form Solutions and Similarity laws." Proc. R. Soc. A, 468, 2294-2318, 2012.
8. Hilber, H. M., T. J. Hughes, R. L. Taylor, "Improved Numerical Dissipation for Time Integration Algorithms in Structural Dynamics," Earthquake Engineering & Structural Dynamics, 5(3):283-292, 1977.
9. Housner, G. W., "The Behavior of Inverted Pendulum Structures during Earthquakes," Bulletin of the Seismological Society of America, 53(2), pp. 403-417, 1963.
10. Kalliontzis, D., S. Sriharan, A. E. Schultz, "Improving Accuracy of the Simple Rocking Model of Rigid Blocks," Proc. 16th World Conf. on Earthquake Engineering, Santiago, Paper No. 451, 2017.
11. Makris, N., Y.S. Roussos, "Rocking Response of Rigid Blocks under Near-Source Ground Motions," Geotechnique, 50(3): 243-262, 2000.
12. Makris, N., M. F. Vassiliou, "Sizing the Slenderness of Free-Standing Rocking Columns to Withstand Earthquake Shaking," Arch Appl Mech, 82:1497-1511, 2012.
13. Milne, J., "Seismic Experiments," Trans. Seismol. Soc. Jpn., 8, 1-82, 1885.
14. Ozer, M., F. Alisverisci, "Dynamic Response Analysis of Rocking Rigid Blocks subjected to Half-Sine Pulse type Base Excitations," Vibration Problems ICOVP 2005, 389-394, 2007 Springer, 2007.
15. Roussis, P.C., S. Odysseos, "Overturning of a Free-Standing Block to a Full-Cycle Seismic Pulse," Proc., 15th World Conf. on Earthquake Engineering, Lisboa, 2012.
16. Vassiliou, M. F., B. Stojadinovic, K. R. Mackie, "A Finite Element Model for Seismic Response Analysis of Deformable Rocking Frames," Earthquake Engng Struct. Dyn., 2016.
17. Zhang, J., N. Makris, "Rocking Response of Free-Standing Blocks under Cycloidal Pulses," J. Eng. Mech., 2001, 127(5): 473-483, 2001.